Available online at website: https://jmes.humg.edu.vn

JOURNAL OF MINING AND EARTH SCIENCES

Volume 66, Issue 4 – 2025

TABLE OF CONTENTS

1. Application of Principal Component Analysis on Seismic Attributes to Predict the Distribution of Early Miocene Reservoirs in the Northeast Bach Ho Muoi Duy Nguyen, Anh Ngoc Le, Ngan Thi Bui, Hong Minh Thi Nguyen, Hang Thu Thi Nguyen	**1**
2. Sand disposal technology selection for oil and gas fields in Malay - Tho Chu basin Quan Anh Tran, An Hai Nguyen, Vinh The Nguyen, Long Khac Nguyen	**11**
3. High-precision coal seam correlation in the Nui Beo mine, North-Eastern Vietnam, using the blood relation algorithm Hung The Khuong, Toan Thi Ta, Hien Thanh Thi Pham	**23**
4. RF-PM_{10}Hybrid Model for Real-Time PM_{10} Forecasting in Open-Pit Copper Mine: A Case Study at the Sin Quyen Copper Mine Ngoc Tuan Le, Hoang Nguyen, Xuan-Nam Bui, Hoa Thu Thi Le	**48**
5. Use two- and three-dimensional models to assess the stability of trench walls for underground construction in sand and sandy silty clay, supported by bentonite suspension Tuong Cat Thi Le, Marek Cała, Agnieszka Stopkowicz, An Phuong Thi Tran	**70**
6. Data-Driven Analysis of Well Logging Data for the Coal Mining Duong Hong Vu, Hung Tien Nguyen, Vinh The Nguyen	**78**
7. Monitoring water volume variations in the Nam Ngum hydropower dam using satellite observations combined with HydroWEB and G-REALM water level data Binh Duc Pham, Hung Manh Nguyen, Teodosio Lacava	**90**
8. The role of online experience in the relationship between customer citizenship behavior and Generation Z loyalty Trung Kien Pham, Chien Van Le, Linh Thuy Thi Phan	**104**

Journal of Mining and Earth Sciences

Website: https://jmes.humg.edu.vn

High-precision coal seam correlation in the Nui Beo mine, North-Eastern Vietnam, using the blood relation algorithm

Hung The Khuong *, Toan Thi Ta, Hien Thanh Thi Pham

Hanoi University of Mining and Geology, Hanoi, Vietnam

ARTICLE INFO

Article history:
Received 02nd Apr. 2025
Revised 01st July 2025
Accepted 04th July 2025

Keywords:
Algorithmic linkage,
Blood relation method,
Coal seam correlation,
Northeastern Vietnam,
Nui Beo mine.

ABSTRACT

The Nui Beo coal mine is located in the Southern region of Quang Ninh province and is part of the Hon Gai-Cam Pha coal field. This formation is acknowledged as one of the most promising coal reserve areas in Vietnam. The blood relation algorithm enables comprehensive synthesis of geological data and systematic processing of stratigraphic parameters, facilitating scientifically robust coal seam identification and correlation. However, applying conventional correlation algorithms in the Quang Ninh coal basin has revealed significant limitations, particularly when distinguishing features-poor coal seams. This study, therefore, introduces an innovative application of the blood relation technique to address these challenges. This method employs parameters, including coal seam thickness, interbedded layers, and angle of incidence. The blood relation technique achieved a correct identification rate of 97.33%, yielding higher efficiency compared to the recurrent neural network-RNN method (84.94%) and logistic regression method (70.87%). Therefore, the application of the blood relation technique for coal seam identification eliminated the need for characteristic factors of the coal seams. The algorithm revealed simpler and more environmentally congruent coal seams in the Nui Beo mine compared to other traditional methods. The findings of this study underscore applied mathematical methods in geological research, emphasize their role in identifying coal seams, and assess their compatibility with the sedimentary environment within the mine.

Copyright © 2025 Hanoi University of Mining and Geology. All rights reserved.

*Corresponding author
E - mail: khuongthehung@humg.edu.vn
DOI: 10.46326/JMES.2025.66(4).03

1. Introduction

Traditionally, the correlation of coal seams has represented a complex issue warranting further scholarly investigation. Existing research in this domain has predominantly focused on stratigraphic correlation and the division of coal seams, emphasizing the critical role of the properties and composition of major elements and trace elements. These pivotal insights have been gleaned through the application of geochemical data processing methodologies, which are largely grounded in the seminal work of Dickinson and Suczek (1979). These methods predominantly utilize the mineral composition of sandstones as a key indicator for determining both the provenance of sedimentary materials and the tectonic setting of the basin.

Empirical research on modern sedimentary basins substantiates that the mineral composition of sandstones varies systematically according to the tectonic setting, correlating functionally with both the origin type and tectonic environment (Potter, 1978; Dickinson & Suczek, 1979; Valloni & Maynard, 1981; Srivastava & Agnihotri, 2013; Zhifei et al., 2019). Such observation is further corroborated by numerous studies focusing on ancient sedimentary basins that affirms the intricate relationship among the mineral composition of sandstones, their provenance and the tectonic framework of the sedimentary basins (Crook, 1974; Schwab, 1975; Dickinson & Suczek, 1979; Dickinson & Valloni, 1980; Dyke et al., 2020; Shi et al., 2020; Li et al., 2021). Consequently, by employing both qualitative and quantitative data analysis techniques, it is possible to determine coal seam correlations using the chemical composition of major oxides, particularly those of rare earth and trace elements.

Sedimentary layers, as well as coal seams, have undergone a relatively continuous development process, establishing a close spatial relationship. Sedimentary layers or coal seams in proximity tend to exhibit similarities in thickness, angles, the number of interbeds, and other characteristics. These shared features serve as the foundation for stratigraphic correlation, coal seam interconnection, and coal seam categorization (Hung, 1996; Einsele, 2020; Duan et al., 2021; Hung et al., 2021, 2022; Hung & Tuyen, 2023; Hou et al., 2023). Following their formation, subsequent tectonic activities cause changes in bedding orientation, the formation of folds, and the displacement of coal seams, resulting in interruptions and complexities within the seam linkage process. Therefore, it is imperative to partition the research area into relatively homogeneous regions to streamline the tasks associated with coal seams and sedimentary layer correlation and linkage.

Most methods of coal seam correlation, which are based on the characteristics of coal seams such as thickness, dip angle, and interbeds, are used for their classification. However, coal seams display significant variations in these attributes and other properties because of their formation in diverse sedimentary environments. To mitigate potential errors, it is customary to partition the coal mining area into homogeneous blocks or distinct regions with relatively similar coal seam characteristics, as evidenced in prior studies (Hung et al., 2021, 2022; Hung & Tuyen, 2023). Various techniques are employed to delineate areas into relatively homogeneous segments, each corresponding to distinct sedimentary environments. These methods include Konstantinov's approach (1968), the Digital Mapping Model (DMM), and K-Means clustering, which is based on Steinhaus's work (1956). Subsequently, classification techniques such as Logistic Regression and Artificial Neural Networks (ANN) are applied to identify coal seams within these uniform zones (Hung et al., 2022). Nevertheless, subdividing the research area into excessively small regions is not considered a viable option due to insufficient training data. Therefore, there may still exist coal seams within the research area that lack homogeneity.

Boreholes placed nearby frequently intersect geological formations that display distinct spatial and temporal correlations. Consequently, the attributes and characteristics of these formations between adjacent boreholes often exhibit notable similarities, effectively representing a familial relationship. Specifically, when pairs of coal seams (compare seam pairs - CSP) in two neighboring boreholes are analyzed, it is apparent that they share a familial connection, akin to siblings, parent-child relationships, or other close

blood relations.

Presently, the coal seam correlation appears in the Nui Beo coal mine, as a whole and more specifically within the Ha Lam coal zone, which is primarily based on the V.7 coal seam. This particular seam typically lies at depths ranging from -300÷350 m and boasts a substantial, relatively stable thickness and dip angle. Consequently, the specifics of coal seam correlation within the mining area are derived from the characteristics of the V.7 coal seam and extended to encompass the seams above and below it. According to Anh (2009), the geological demarcation between the Nui Beo and Ha Lam mines is marked by anticline 158. Although these mines share the same coal seam, they exhibit distinct geological features. The Nui Beo coal mine includes the V.12 coal seam, albeit discontinuous, with a thickness fluctuating around 1.0 m, whereas the Ha Lam mine rarely encounters the V.12 coal seam. The Nui Beo mine encompasses nearly all coal seams from V.14 down to V.4 seams, while the Ha Lam one includes V.11 and lower coal seams and excludes V.14, V.13, and V.12 seams. Moreover, below the V.7 coal seam in Nui Beo, additional seams such as V.6 coal seam (although relatively thin, approximately 1.0 m thick and discontinuous), V.5, V.4, and further down, sedimentary layers associated with the Hon Gai formation are encountered. Conversely, in the Ha Lam mine, only the V.7 coal seam is present, followed by direct contact with the Carboniferous-Permian limestone of the Ha Long formation. Accordingly, discrepancies in stratigraphic order and coal seam sequence are evident even within the same Ha Lam coal zone, reflecting the intricacies and challenges in geological research in the entire mining area, especially regarding coal seam correlation and grouping. The objective of this study is to identify coal seams in the Nui Beo area, Quang Ninh province, by applying the blood relation (BLR) algorithm. The methodology involves analyzing key parameters, including seam thickness, dip angle, interbeds, and coal quality. This will serve the purpose of coal seam correlation and grouping, ultimately contributing to the precise and suitable design of mining operations that align with the specific mining conditions in the area.

2. General geological background of the Nui Beo mine

The Nui Beo mine is situated in Ha Long city, Quang Ninh province, approximately 4 km southwest of Ha Long City Centre, on the left side of National Highway 18A leading from Ha Long to Mong Duong areas (Figure 1A). Within the mining site, there are Triassic sediments belonging to the Hon Gai formation, specifically its middle sub-formation, along with loose deposits from the

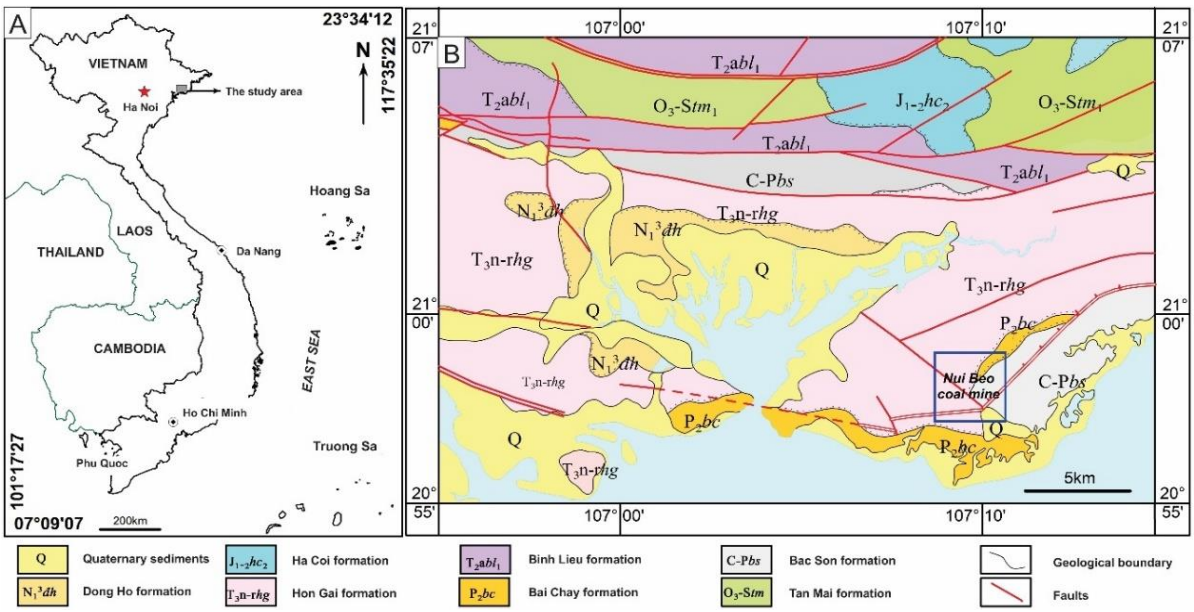

Figure 1. A-Sketch map of Vietnam and the location of the study area and B-Geological map of Ha Long area showing the location of the Nui Beo mine (Hung, 1996).

Quaternary system (Figure 1B) (Hung, 1996). The middle Hon Gai sub-formation exhibits a petrographic composition of alternating siltstone, sandstone, claystone, coal clay, and coal seams, with a total stratigraphic thickness of approximately 1,800 m. Notably, this sub-formation contains economically significant industrial coal seams (Figure 2).

Quaternary sediments are found directly overlaying the middle Hon Gai formation, extending across lower-lying regions and valleys surrounding the Nui Beo mine. These sedimentary compositions consist of pebbles, gravels, sands, loose clay, occasional rolling boulders, and weathering products derived from pre-existing rocks.

The Nui Beo mine area exhibits a complex geological terrain characterized by folds and fault systems, which pose significant challenges in identifying coal seams and conducting efficient coal mining operations. As stated by Anh (2009), when descending from the surface terrain within the mine, the following coal seams can be identified, they are V.14, V.13, V.11, V.10, V.9, V.7, V.6, V.5, and V.4 coal seams.

3. Materials and methods

3.1. Data collection

Data for this study were derived from 223 boreholes drilled in the Nui Beo coal mine, capturing essential parameters such as seam thickness, dip angle, and interbedded layers. Additionally, 438 laboratory analyses provided data on moisture content, ash content, volatile matter, and calorific value. Key sources included exploration reports from the Ha Lam coal mine (Anh, 2009; Hung, 2019) and new drilling records from deeper sections of the Nui Beo mine.

3.2. Blood relation algorithm (BLR)

3.2.1. Basis of the method

Boreholes encountering coal seams are akin to barcodes, with each barcode possessing a set of characteristics and properties, including coal thickness, dip angle, and the number of coal layers. The comparison process involves superimposing these barcodes to minimize discrepancies between them through the application of various techniques, such as the compare seam pairs (CSP) method. This method exhibits similarities to genetic analysis, barcode scanning, quick response code (QR code), and face recognition methods. The outcomes of these comparisons facilitate the linking of coal seams.

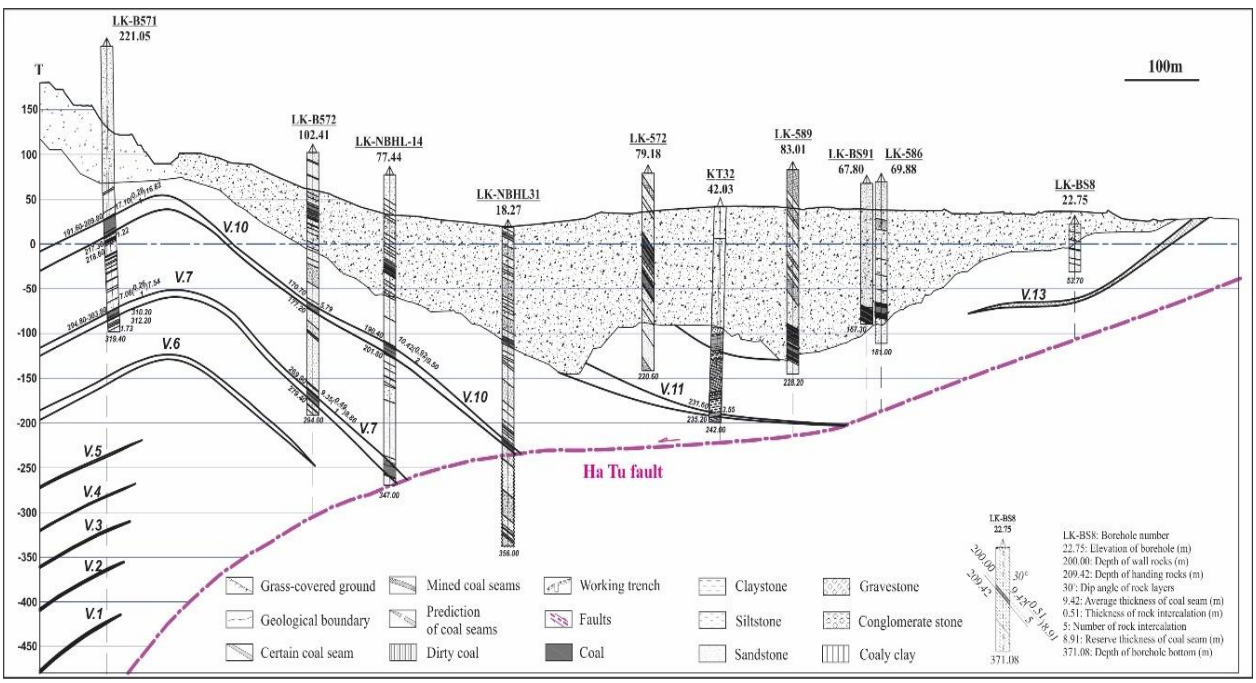

Figure 2. Geological cross-section of line T.VA showing the coal seams and structure of the Nui Beo mine (Anh, 2009; Hung, 2019).

If the comparison between the LKA and LKD boreholes is taken into consideration, the likelihood of accurately determining corresponding seams between these two boreholes diminishes when contrasted with the comparison between the LKB and LKC boreholes (Figure 3). This demonstrates that spatial proximity between boreholes enhances the similarity of seam characteristics, facilitating more reliable correlation and yielding more precise results when analyzing closely spaced boreholes. In contrast, as boreholes become more distant from each other, the properties of the coal seams also exhibit variations. Therefore, employing conventional mathematical methods for ascertaining specific characteristics of each seam has become a challenging endeavor. To mitigate errors in seam correlation, it is important to factor in the distance between the research borehole and the standard borehole, opting for the nearest borehole as the basis for comparison. Consequently, the focus transitions from identifying coal seams in relatively homogeneous regions to scrutinizing two closely spaced boreholes. In this context, the BLR method or the compare seam pairs method is selected for implementation.

Due to dynamic processes within the Earth's crust, certain regions experience uplift followed

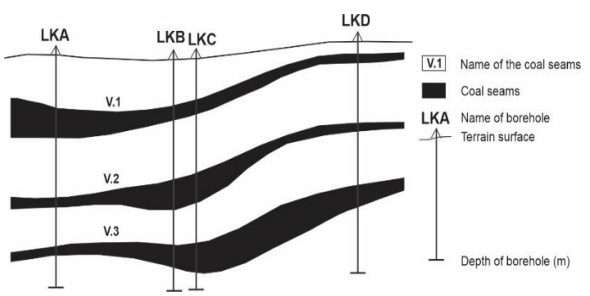

Figure 3. Comparison of adjacent borehole pairs.

by subsequent weathering or erosion, resulting in the loss of coal seams. Moreover, within the same basin or depression, identical coal seams can originate in diverse environments, including tidal flats, riverine settings, or estuaries, leading to frequent discontinuities in coal seam formation. Accordingly, the challenge of controlling the comparison distance arises. This distinction sets the method apart from AND methods, barcode methods and face recognition techniques. To ensure the seam pair comparison method yields accurate results, it is crucial to select cases for comparison that are as similar as possible, thereby minimizing comparison errors. This principle lies at the core of the seam pair comparison method.

This comparison is based on the characteristics of the nearest boreholes, akin to familial relationships such as siblings or parent-child connections, and extends to adjacent boreholes along specific cross-sections. The methodology requires first establishing a standard borehole that exhibits a well-defined stratigraphic sequence encompassing all coal seams from top to bottom. The analysis demonstrates that spatial proximity strongly influences the degree of similarity between boreholes-closer boreholes exhibit more comparable characteristics and properties, representing what we term a "blood relationship". In contrast, more distant boreholes show progressively weaker blood relationships. This geological concept, while analogous to biological familial relationships in some respects, operates on fundamentally different principles than those observed in plant and animal systems.

The BLR method encompasses various forms, including (Figure 4): 1) Method for determining the random relationship which involves the comparison of any two boreholes; 2) Method for determining the relationship to the center which entails comparing neighboring boreholes to a central borehole; 3) Method for determining the

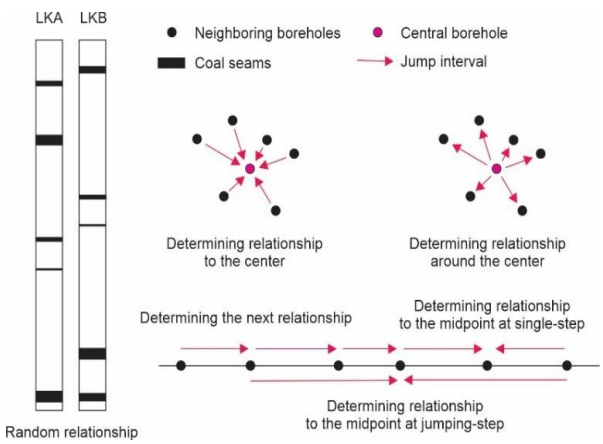

Figure 4. Method for determining the next relationship.

relationship around the center which relies on the central borehole as a reference point and identifies adjacent boreholes in its vicinity; 4) Method for determining the next relationship which is primarily employed in cross-section analysis. It entails comparing a new borehole to establish the subsequent standard borehole and consistently follows a single-step approach, and finally 5) Method for determining the relationship to the midpoint on the cross-section, which entails comparing boreholes at either single-step or jump-wise intervals along the cross-section.

The central technique within the BLR approach is understood as the method for determining the next relationship. Additional methods, such as determining the random relationship, relationship to center, relationship around center, relationship to midpoint with a single step, and relationship to midpoint with a jump step, are used to corroborate the outcomes derived from the primary method (Figure 4). Following implementation, corrective adjustments are made to address any identification errors. The correlation process may encounter several geological challenges, including the absence of coal seams, fault-disrupted seams, eroded seams, or displaced seams. To ensure identification accuracy, such problematic seams may be selectively excluded from the analysis. This quality control measure helps minimize misidentification while maintaining the integrity of the correlation results.

3.2.2. Method for comparing seam pairs (CPS)

Initially, a comparison between the LKA and LKB boreholes was conducted that corresponded to three coal seams as depicted in Figure 5. It is revealed from the findings that there is an absence of alignment. By adjusting the LKB borehole downward, it is evident that the AV2 coal seam from the LKA borehole aligns with the BV1 coal seam of the LKB borehole, demonstrating a significant overlap. This method of comparison bears resemblance to the techniques used in DNA sequencing or barcode matching.

It is assumed that the LKA borehole encompasses m_1 coal seams, while the LKB borehole has m_2 coal seams. These coal seams can be likened to tags embedded with barcodes, where each stripe represents a distinct coal seam.

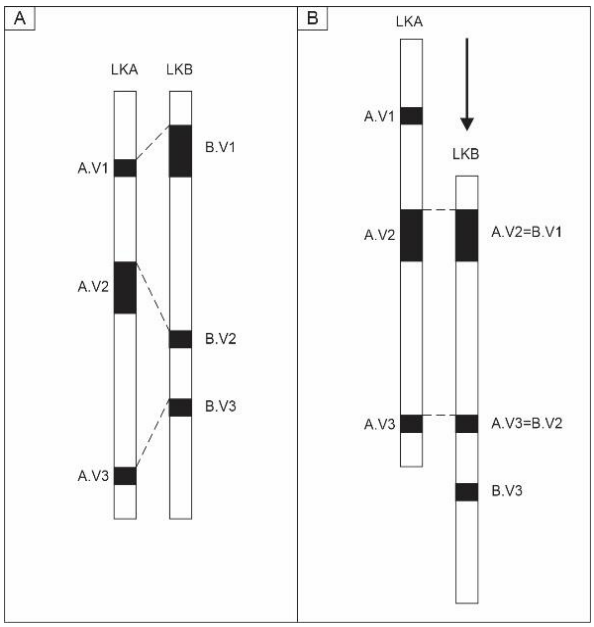

Figure 5. Method of comparing seam pairs (CSP): A - Asynchronous comparison case; B - Synchronous comparison case.

Each stripe provides details about its coordinate position, thickness of the coal seam, inclination angle, and number of interbedded layers.

It is important to adjust the lines vertically to align their properties and characteristics as closely as possible. Consequently, the challenge is to determine a position where the deviation (δ) between comparative parameters is minimized.

a. Deviation (δ)

Depending on the context, the deviation can be determined using either the absolute difference or the squared difference between two values. For the assessment of deviation among coal seam parameters, the absolute difference is employed (Eq. 1).

$$\delta = \frac{1}{m}\sum_{i=1}^{m} | x_i - y_i | \qquad (1)$$

where: δ represents the absolute deviation; x_i and y_i denotes the values of the ith parameter for boreholes x and y, respectively. m stands for the number of parameters being compared. Given the variation in units of measurement across these parameters, normalization of each parameter's value is crucial before any computation.

Furthermore, the comparative scope must be carefully evaluated. When analyzing five coal seam pairs versus two pairs, the absolute cumulative difference will naturally be greater for the larger set. To enable meaningful comparison, it is therefore necessary to normalize the results by calculating the average difference per pair. This normalized value can be determined using equation (2).

$$\delta = \frac{1}{v}\sum_{i=1}^{v} | X(i) - Y(i) | \quad (2)$$

where: δ is the error, *X(i)* and *Y(i)* are the values of seam i, and *v* is the number of seam pairs being compared.

Considering that the seam pairs are not uniformly aligned based on their parameters, it is limited to selecting *t* pairs for comparison. Consequently, formula (2) is elaborated further as equation (3).

$$\delta = \frac{1}{v \times t}\sum_{i=1}^{v} | X(i) - Y(i) | \quad (3)$$

where: *t* is the number of synchronized pairs.

b. Thickness of the sedimentary rock layer (M)

The thickness of sedimentary rock layers (*M*) serves as a critical parameter in coal seam correlation. While coal seam thickness may exhibit significant variation between proximal boreholes - particularly due to rapid seam thinning - the intervening sedimentary rock layers maintain remarkable consistency in thickness (Figure 6). This stability reflects the greater temporal persistence of sedimentary deposition processes compared to the more variable conditions governing peat accumulation and coal formation. As such, sedimentary rock layer thickness provides a more reliable correlative benchmark than coal seam thickness alone and is consequently employed as a constant reference parameter in seam identification.

Hence, the significance of sedimentary rock layer thickness becomes more pronounced when contrasting the thicknesses of coal seams. To optimize the application of this sedimentary rock layer thickness coefficient, one employs an additional metric known as the similarity coefficient (alternatively referred to as the equivalence/difference coefficient - *Kg*).

c. Similarity coefficient (Kg)

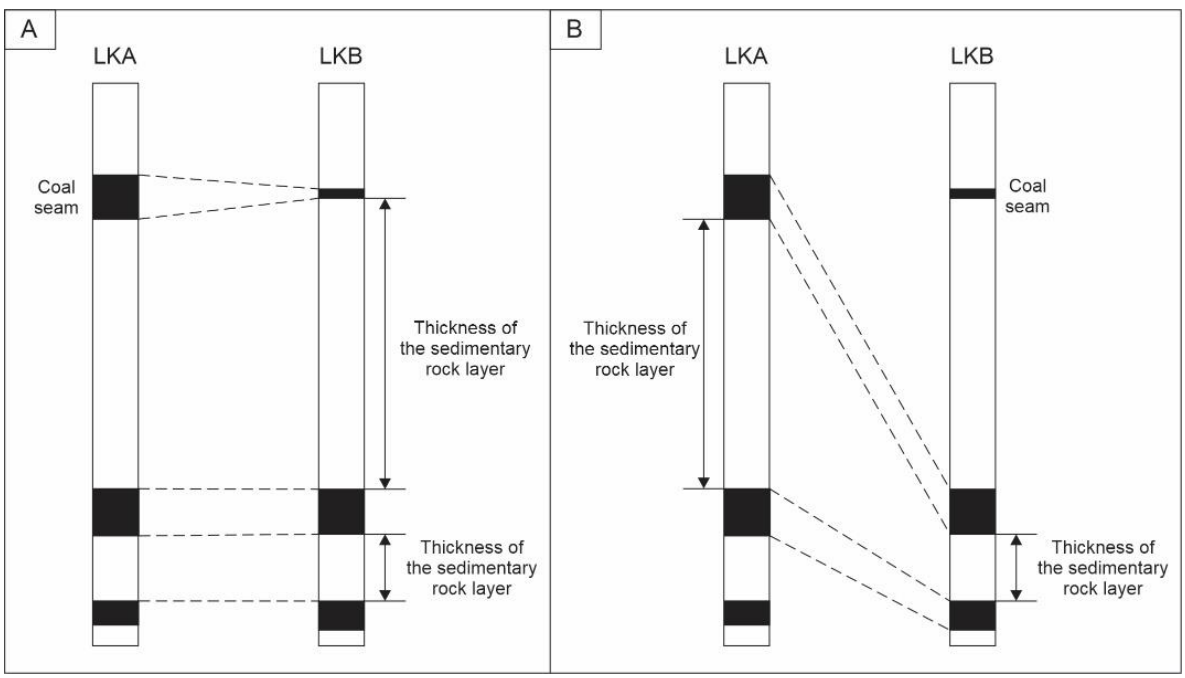

Figure 6. A comparison of sedimentary rock layer thickness (M) in various cases; A - Disparate coal seam thicknesses with consistent sedimentary rock layer thickness; B - Uniform coal seam thickness with varying sedimentary rock layer thickness.

To better bring out the differences among features during the comparison process, coefficients indicating similarity or dissimilarity are incorporated. These similarity coefficients function as weights, thereby elevating the significance of the research parameters. The similarity coefficient (*Kg*) is calculated using equation (4).

$$Kg = \frac{GT_{max}}{GT_{\min}} \quad (4)$$

where: *Kg* is the similarity coefficient and GT_{min} and GT_{max} are the minimum and maximum values at the comparison position of the two LKA and LKB boreholes, respectively.

The coefficient *Kg* invariably exceeds 1.0, with values approaching 1.0 denoting increased similarity between two coal seams. Conversely, a higher *Kg* reflects a greater disparity between the seams. Thus, the similarity coefficient *Kg* amplifies the value of comparison. When equation (4) is utilized to compare the total thicknesses at two boreholes, it is termed the total thickness similarity coefficient (Kg_T). Nonetheless, since the GT_{min} value for certain coal seams may be zero, equation (4) can be reformulated as depicted in equation (5).

$$Kg_T = \frac{GT_{\max}}{\left(\frac{GT_{\min} + GT_{max}}{2}\right)} = \frac{2 \times GT_{max}}{GT_{\min} + GT_{max}} \quad (5)$$

The similarity coefficient (Kg_T) functions serves as an error-correction factor in correlation analysis. Although its application remains discretionary for certain comparative assessments, this coefficient becomes essential when evaluating total thickness comparisons between coal seams.

d. Geometric factor (K_{hh})

During the coal seam correlation process, the foremost criterion is to prioritize the connection of seams possessing equivalent elevations. Viewed geometrically, it is impractical to link a coal seam present at the surface of one borehole with a seam located at the bottom of a different borehole and vice versa (Figure 7).

Fundamentally, the geometric factor (K_{hh}) is seen as a methodology pertaining to seam geometry, long employed by geologists during the coal seam correlation process. Within this algorithm, the notion of a geometric factor, denoted as $K_{hh,}$ is introduced. This coefficient serves to express the equivalence between connected coal seams with respect to their height. When two coal seams are of equal height, the K_{hh} coefficient is zero. Conversely, as the height differential between the seams increases, so does the K_{hh} coefficient (Figure 7). This concept is analogous to the tan(α) value of the angle, which is created by the line connecting the coal seams and the horizontal plane (Eq. 6).

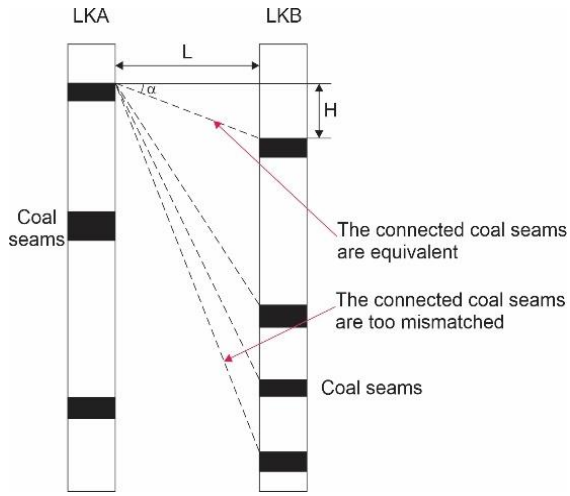

Figure 7. Application of geometric factor (K_{hh}) to connected coal seams.

$$K_{hh} = \tan(\alpha) = \frac{H}{L} = \frac{|Y_2 - Y_1|}{|X_2 - X_1|} \quad (6)$$

where: K_{hh} - Geometric factor, α - Angle between the line connecting the seams and the horizontal plane (degree), *H* - Height difference (m), *L* - Distance between two boreholes (m); X_1, X_2 - the coordinates of the coal seam along the horizontal axis (m); Y_1, Y_2 - the coordinates of the coal seam along the vertical axis (m).

Employing the geometric factor (K_{hh}) for connecting coal seams can incur errors, especially when the seams undergo displacement due to faulting or folding, yielding a pronounced slope within the seam. In light of this, an alternative parameter is necessary for these situations. Hence, an error term, denoted as Δ, is suggested and can be computed using formula (7).

$$\Delta = \frac{1}{m+2}\sum_{j=1}^{m+2}\frac{1}{v\times t}\sum_{i=1}^{v} Kg_T \times Kg \times |X(i,j) - Y(i,j)| \quad (7)$$

Where: Δ represents the error term; *X(i,j)* and *Y(i,j)* are the values of seam i at parameter j; ν is the number of compared seam pairs; t is the number of pairs with synchronized parameters; m is the number of parameters; *Kg* is the similarity coefficient for each parameter. If *Kg*=1, then Kg_T is the similarity coefficient for sedimentary rock layer thickness - this coefficient is applicable only to rock layers; other parameters have Kg_T=1. m represents the number of parameters involved in the comparison; m+1 corresponds to the geometric factor (K_{hh}) and m+2 corresponds to the thickness of the sedimentary rock layer (*M*).

It is important to highlight that when the comparison of coal seams is conducted with the use of the BLR algorithm, errors (*Δ*) aligning with either of the two geometric coefficients (K_{hh}) or the rock sedimentary layer thickness (*M*) should be prioritized. If the error does not align with either of these parameters, it is recommended to select an error that falls within the intermediate range between the geometric coefficient and the rock sedimentary layer thickness.

When a borehole intersects faults or folds, the errors in comparing the coal seam (Δ), can be substantial. To choose the appropriate method for coal seam comparison, both the sedimentary rock layer coefficient (*M*) and the geometric coefficient (K_{hh}), should be taken into consideration.

4. Results and Discussion

4.1. Coal seam characteristics

The Nui Beo coal mine is partitioned into relatively homogeneous areas, each corresponding to distinct formative environments: Area A1 exhibits characteristics of swamp conditions; Areas A2 and A3 are tidal flats; Area B is indicative of a flow environment; Area C is another tidal flat; Area D is characterized as a swamp and Area E represents a peripheral area (Hung et al., 2022; Hung and Tuyen, 2023). The F-Monplane fault demarcates areas A1 and A2, with subgroup factors determining the boundary between them. Areas B and A are separated by the F-K and F-C faults, accompanied by a steep gradient. The manifestation of flows through area B delineates it from area C. A significant slope marks the boundary between areas D and C, while area E is distinct and demarcated by the F-N fault (Figure 8). This configuration underscores the complexity of coal seam formation in the Nui Beo coal mine, highlighting the presence of coal seams that have formed in a variety of sedimentary environments. This phenomenon is crucial in the process of correlating and linking coal seams in the mine.

Based on three obtained parameters of coal seams from boreholes, such as angle of incidence, actual thickness, and number of interbedded layers, it is feasible to evaluate these parameters with enhanced reliability. This evaluation is achieved using correlation coefficients and the

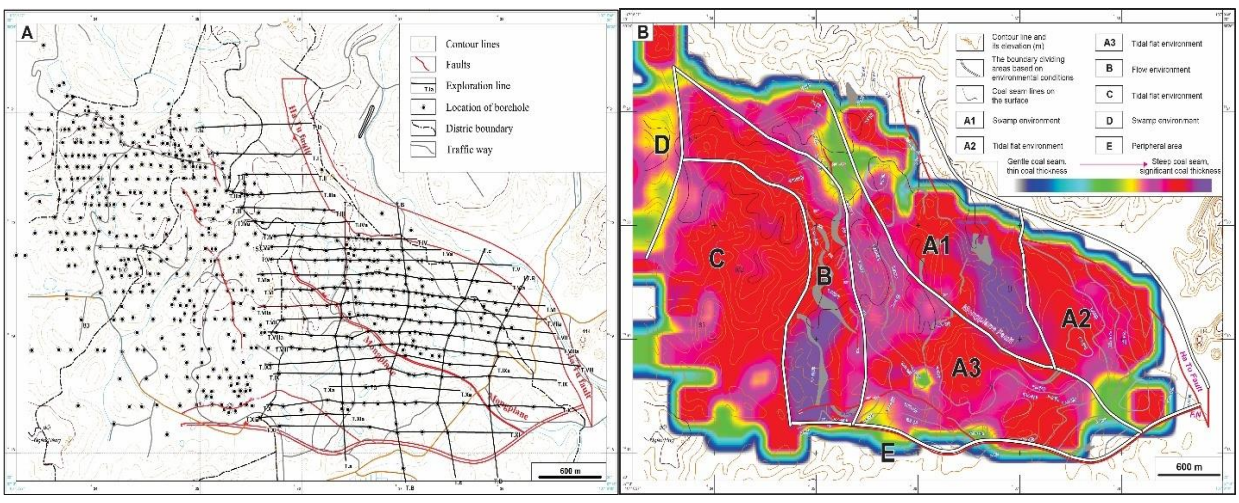

Figure 8. A - Sketch map of the Nui Beo mine and locations of coal exploration boreholes; B - Dividing the Nui Beo coal mining areas based on coal-forming environments (Hung et al., 2022; Hung and Tuyen, 2023).

amount of information (Freedman, 2009; Hung et al., 2021), as presented in Table 1.

Table 1. Evaluation of the drilling parameters and correlation coefficients between them.

Parameters	Angle of incidence	Actual thickness	Interbedded layers
Angle of incidence	1	-0.051	-0.041
Actual thickness	-0.051	1	0.741
Interbedded layers	-0.041	0.741	1
Order	Actual thickness	Interbedded layers	Angle of incidence
Amount of information	60.52%	82.84%	100%

Seam thickness and interbedded layers demonstrated high stability across boreholes, supporting their reliability for seam correlation (Table 1). Variations in dip angles are closely associated with tectonic influences. An inverse relationship is found between the actual thickness of coal seams and their angle of incidence, with a correlation coefficient of R_{xy}=-0.051 (Table 1). Specifically, as the thickness of a coal seam increases, its angle of incidence decreases. Conversely, thinner coal seams tend to have a steeper angle of incidence. This observed correlation suggests that major structural disturbances, such as faulting or folding capable of substantially elevating or depressing coal seams, were relatively uncommon during seam formation within the basin environment. Such patterns show that parameters such as angle of incidence, seam thickness, and the number of interbedded layers is valuable for comparing and identifying different coal seams. Furthermore, the analysis reveals that seam thickness is the most reliable parameter, accounting for 60.52% of the variance, followed by the number of interbedded layers and then the angle of incidence.

4.2. Identifying coal seams based on the BLR method, case study NBHL38 and NBHL24 boreholes

To identify coal seams, it is essential to first select a standard borehole for comparison. Regarding this study, the chosen borehole is the NBHL38 due to its notably stable stratigraphy based on specific requirements. Furthermore, mathematical methods utilized for coal seam identification, including K-means, logistic regression, and recurrent neural network (RNN), produce mutually consistent results that show strong agreement with conventional contouring method outcomes (Table 2) (Hung et al., 2022; Hung and Tuyen, 2023).

Along the T.VIIA cross-section line, a comparative analysis is undertaken between the NBHL24 borehole and the standard NBHL38 borehole. The parameters on the NBHL24 borehole are presented in the summary below (Table 3).

Table 2. Comparative parameters for the NBHL38 borehole on the T.VIIA cross-section line.

Coal seam according to the original document(1)	Coal seams in descending order	Coordinates of the coal seam in cross-section		Angle of incidence (degree)	Actual thickness (m)	Interbedded layers
		X (m)	Y (m)			
V.13	1	1960	1148			
V.11	2	1961	1087	10	4.33	1
V.10	3	1962	1023	10	5.22	1
V.9	4	1964	924	10	6.89	1
V.7	5	1965	816	10	10.54	1
V.6	6	1967	762	10	2.75	1
Note: (1) - The coal seam is identified through a comprehensive report that amalgamates data from Anh (2009).						

Table 3. Comparative parameters of coal seams for the NBHL24 borehole on the T.VIIA cross-section line.

Coal seam, according to the original document(1)	Coal seams in descending order	Coordinates of the coal seam in cross-section		Angle of incidence (degree)	Actual thickness (m)	Interbedded layers
		X (m)	Y (m)			
V.13	1	1760	1127	15	3.28	0
V.11	2	1760	1062	15	5.99	1
V.10	3	1760	995	15	6.58	1
V.9	4	1761	897	15	7.92	0
V.8	5	1761	873			
V.7	6	1762	785	15	11.98	1
V.6	7	1762	736	15	3.87	1
V.5	8	1762	718			

In an analysis of 13 comparative instances, the coal seams from the standard NBHL38 borehole were shifted and juxtaposed against those of the NBHL24 borehole. Notably, in the eighth instance (8:1//1), the first coal seam in the NBHL38 borehole, which corresponds to coal seam V.13, aligns with the first coal seam (V.13) in the NBHL24 borehole. The observed error in this comparison amounts to 0.050, marking the minimal discrepancy (Table 4). It is suggested from this observation that the sequential coal seams from the uppermost to the lowermost in the NBHL24 borehole align with the V.13, V.11, V.9, V.7, and V.6 coal seams in the standard NBHL38 borehole. It is important to note that since the NBHL38 borehole lacks the V.8 coal seam, to ensure accuracy in seam linkage, the corresponding V.8 coal seam in the NBHL24 borehole has been excluded from consideration (Table 5).

The calculation process is iteratively repeated multiple times until it enables the determination of corresponding coal seams for the boreholes being compared (Table 6).

The correlation analysis follows a sequential approach along the T.VIIA cross-section. An initial comparison is made between the standard borehole NBHL38 and borehole NB75. This pairwise evaluation then progresses systematically to adjacent boreholes until all boreholes along the T.VIIA transect have been analyzed (Appendix 1, Figure 9). Furthermore, borehole NBHL38 will also be analyzed concerning nearby boreholes located on other cross-sections, such as borehole 100 (Appendix 2).

The comparison between the standard borehole NBHL38 and adjacent borehole NB75 demonstrates the following coal seam characteristics (Appendix 3, Figure 10). Quantitative analysis reveals that both Case 4 and Case 5 exhibit minimal error rates (0.065). However, further examination of geometric parameters reveals that Case 4 exhibits a significantly lower geometric coefficient (K_{hh}=0.026) compared to Case 5 (K_{hh}=0.085). On the other hand, the coefficient about the sedimentary rock layer (M) is markedly higher in case 4 (M=0.045) compared to case 5 (M=0.014) (Appendix 4). As previously established, the M coefficient holds greater diagnostic weight for coal sedimentation analysis compared to the geometric coefficient (K_{hh}). Consequently, Case 5 has been selected as the optimal basis for equivalent coal seam correlation (Appendix 5 & 6).

The analytical results demonstrate that coal seam 1 in borehole NB75 correlates with coal seam 2 in the standard borehole NBHL38. This established correlation serves as the basis for subsequent seam identification throughout the study area (Appendix 5). However, when comparing seams in a descending stratigraphic order, similar lithological properties between adjacent seams may lead to potential misidentification. To mitigate this, it is advisable to utilize the minimal rock layer thickness coefficient as a distinguishing criterion. Since the coefficient of geometric similarity (K_{hh}) plays a pivotal role in determining the relational formation of coal seams, any margin of error

introduced must cater to the minutest discrepancies in the coal seams.

Table 4. Results of the error assessment between the NBHL38 and NBHL24 boreholes.

Cases for comparison	Geometric Factor (K_{hh})	Sedimentary rock layer factor (M)	Angle of incidence (degree)	Actual thickness (m)	Interbedded layers	Error (Δ)
1:1//8	2.172					2.172
2:1//7	0.984	0.922	0.500	0.500	0.500	0.681
3:1//6	0.569	0.208	0.200	0.176	0.167	0.264
4:1//5	0.335	0.121	0.117	0.135	0.083	0.158
5:1//4	0.197	0.153	0.120	0.134	0.100	0.141
6:1//3	0.104	0.075	0.087	0.101	0.100	0.093
7:1//2	0.057	0.040	0.060	0.055	0.067	0.056
8:1//1	0.025	0.035	0.060	0.066	0.067	0.050
9:2//1	0.067	0.041	0.072	0.055	0.120	0.071
10:3//1	0.170	0.069	0.050	0.063	0.125	0.095
11:4//1	0.369	0.073	0.067	0.116	0.111	0.147
12:5//1	0.742	0.056	0.100	0.224	0.250	0.274
13:6//1	1.763		0.200	0.088	1.000	0.763
Note: 1:1//8 - First comparison case: Comparing coal seam 1 in the standard borehole to (//) coal seam 8 in the comparative borehole (Coal seam 1 in the NBHL38 borehole compared to (//) coal seam 8 in the NBHL24 borehole).						

Table 5. Results of the comparative parameters between the NBHL38 and NBHL24 boreholes.

No	Standard borehole (exploration line)	Comparing borehole (exploration line)	Geometric factor (K_{hh})	Standard// Comparing (*)	Sedimentary rock layer factor (M)	Standard// Comparing (**)	Error (Δ)	Standard// Comparing (***)	Results
1	NBHL38 (T.VIIA)	NBHL38 (T.VIIA)	0	1//1	0	1//1	0	1//1	1//1
2	NBHL38 (T.VIIA)	NBHL24 (T.VIIA)	0.025	1//1	0.035	1//1	0.050	1//1	1//1
Note: * - Comparison case based on the smallest geometric factor (K_{hh}); ** - Comparison case based on the smallest sedimentary rock factor (M); *** - Comparison case based on the smallest error (Δ).									

Table 6. Results from forecasting the coal seams in the NBHL24 borehole.

No	Exploration line	Borehole	Coal seam according to the original document(1)	Coordinates of the coal seam in cross-section		Forecasting the coal seam
				X (m)	Y (m)	
1	T.VIIA	NBHL24	V.13	1760	1127	V.13
2	T.VIIA	NBHL24	V.11	1760	1062	V.11
3	T.VIIA	NBHL24	V.10	1760	995	V.10
4	T.VIIA	NBHL24	V.9	1761	897	V.9
5	T.VIIA	NBHL24	V.8	1761	873	V.8
6	T.VIIA	NBHL24	V.7	1762	785	V.7
7	T.VIIA	NBHL24	V.6	1762	736	V.6
8	T.VIIA	NBHL24	V.5	1762	718	V.5

Appendix 1. Results of the comparative parameters between the NBHL38 borehole and neighboring boreholes.

No	Standard borehole (exploration line)	Comparing borehole (exploration line)	Geometric factor (K_{hh})	Standard// Comparing (*)	Sedimentary rock layer factor (M)	Standard// Comparing (**)	Error (Δ)	Standard// Comparing (***)	Results
1	NBHL38 (T.VIIA)	NBHL38 (T.VIIA)	0	1//1	0	1//1	0	1//1	1//1
2	NBHL38 (T.VIIA)	100 (T.VI)	0.031	1//1	0.029	1//1	0.063	1//1	1//1
3	NBHL38 (T.VIIA)	NB58 (T.VIA)	0.038	1//1	0.012	2//1	0.067	1//1	2//1
4	NBHL38 (T.VIIA)	NBHL24 (T.VIIA)	0.025	1//1	0.035	1//1	0.050	1//1	1//1
5	NBHL38 (T.VIIA)	NBHL28 (T.VIIIA)	0.017	1//2	0.008	1//2	0.041	1//2	1//2
6	NBHL38 (T.VIIA)	NB75 (T.VIIA)	0.026	1//1	0.014	2//1	0.065	2//1	2//1

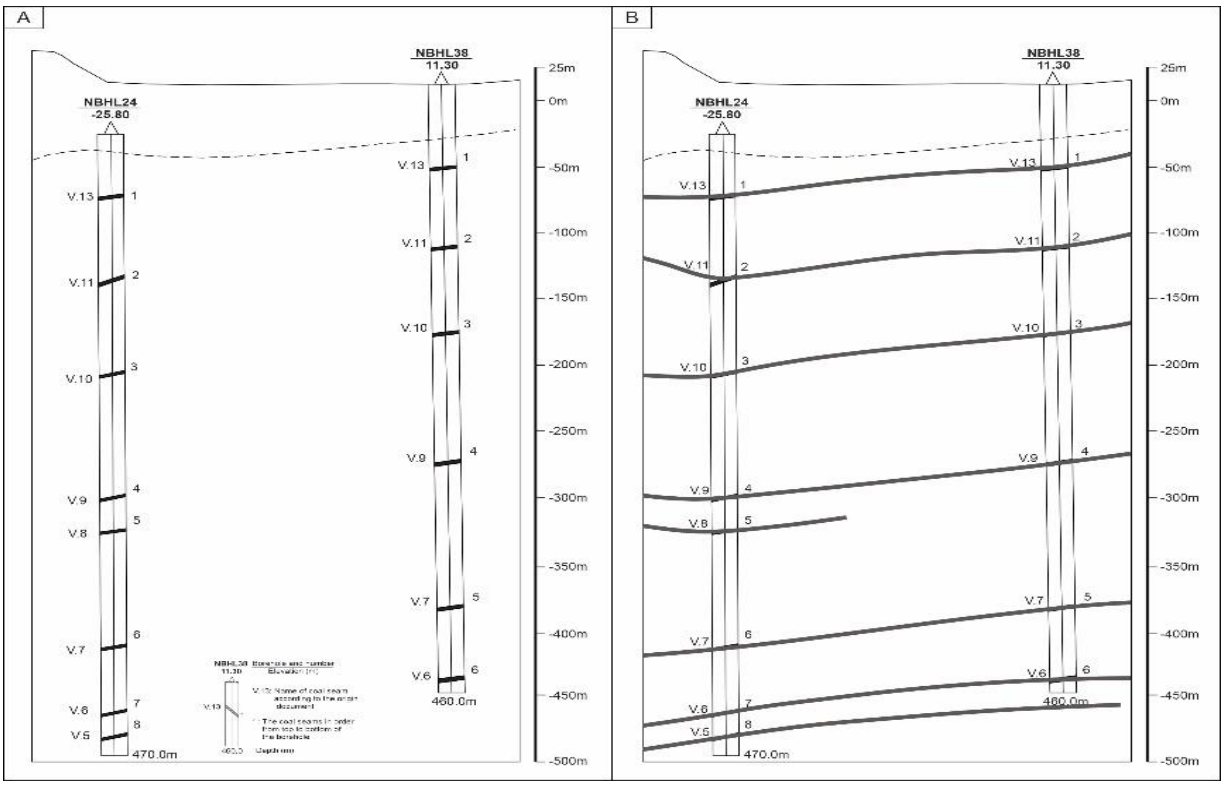

Figure 9. Comparison between the NBHL38 (standard) and NBHL24 (comparison) boreholes conducted along the T.VIIA cross-section line. A - Examination of the stratigraphy and the sequence of coal seams within the stratigraphic columns of the NBHL38 and NBHL24 boreholes; B - Establishing coal seam connections utilizing the computational results obtained from the algorithm.

Appendix 2. Results from forecasting the coal seams in neighboring the NBHL38 borehole.

No	Exploration line	Borehole	Coal seam according to the original document(1)	Coordinates of the coal seam in cross-section		Forecasting the coal seam
				X (m)	Y (m)	
1	T.VIIA	NBHL38	V.13	1960	1148	V.13
2	T.VIIA	NBHL38	V.11	1961	1087	V.11

3	T.VIIA	NBHL38	V.10	1962	1023	V.10
4	T.VIIA	NBHL38	V.9	1964	924	V.9
5	T.VIIA	NBHL38	V.7	1965	816	V.7
6	T.VIIA	NBHL38	V.6	1967	762	V.6
7	T.VI	100	V.13	1833	1170	V.13
8	T.VI	100	V.11	1833	1099	V.11
9	T.VI	100	V.10	1833	1025	V.10
10	T.VIA	NB58	V.11	2123	1178	V.11
11	T.VIA	NB58	V.10	2124	1111	V.10
12	T.VIA	NB58	V.9	2128	1021	V.9
13	T.VIIA	NBHL24	V.13	1760	1127	V.13
14	T.VIIA	NBHL24	V.11	1760	1062	V.11
15	T.VIIA	NBHL24	V.10	1760	995	V.10
16	T.VIIA	NBHL24	V.9	1761	897	V.9
17	T.VIIA	NBHL24	V.8	1761	873	V.8
18	T.VIIA	NBHL24	V.7	1762	785	V.7
19	T.VIIA	NBHL24	V.6	1762	736	V.6
20	T.VIIA	NBHL24	V.5	1762	718	V.5
21	T.VIIIA	NBHL28	V.14	1800	1167	V.14
22	T.VIIIA	NBHL28	V.13	1800	1129	V.13
23	T.VIIIA	NBHL28	V.11	1802	1075	V.11
24	T.VIIIA	NBHL28	V.10	1804	1006	V.10
25	T.VIIIA	NBHL28	V.9	1806	916	V.9
26	T.VIIIA	NBHL28	V.7	1810	806	V.7
27	T.VIIA	NB75	V.11	2243	1197	V.11
28	T.VIIA	NB75	V.10	2243	1123	V.10
29	T.VIIA	NB75	V.9	2245	1009	V.9
30	T.VIIA	NB75	V.7	2247	903	V.7

Appendix 3. Comparative parameters for the NB75 borehole on the T.VIIA cross-section line.

Coal seam according to the original document(1)	Coal seam in descending order	Coordinates of the coal seam in cross-section		Angle of incidence (degree)	Actual thickness (m)	Interbedded layers
		X (m)	Y (m)			
V.11	1	2243	1197	30	5.46	2
V.10	2	2243	1123	25	5.35	0
V.9	3	2245	1009	25	7.26	1
V.7	4	2247	903	25	9.88	2

Appendix 4. Results of the error assessment between the NBHL38 and NBHL75 boreholes.

Cases for comparison	Geometric factor (K_{hh})	Sedimentary rock layer factor (M)	Angle of incidence (degree)	Actual thickness (m)	Interbedded layers	Error (Δ)
1:1//4	0.854					0.854
2:1//3	0.283	0.234	0.214	0.195	0.167	0.219
3:1//2	0.087	0.161	0.143	0.094	0.056	0.108
4:1//1	0.026	0.045	0.107	0.037	0.111	0.065
5:2//1	0.085	0.014	0.112	0.012	0.104	0.065
6:3//1	0.158	0.047	0.112	0.056	0.104	0.095
7:4//1	0.330	0.105	0.151	0.099	0.148	0.167
8:5//1	0.670	0.107	0.232	0.160	0.333	0.300
9:6//1	1.576		0.500	0.330	0.333	0.685

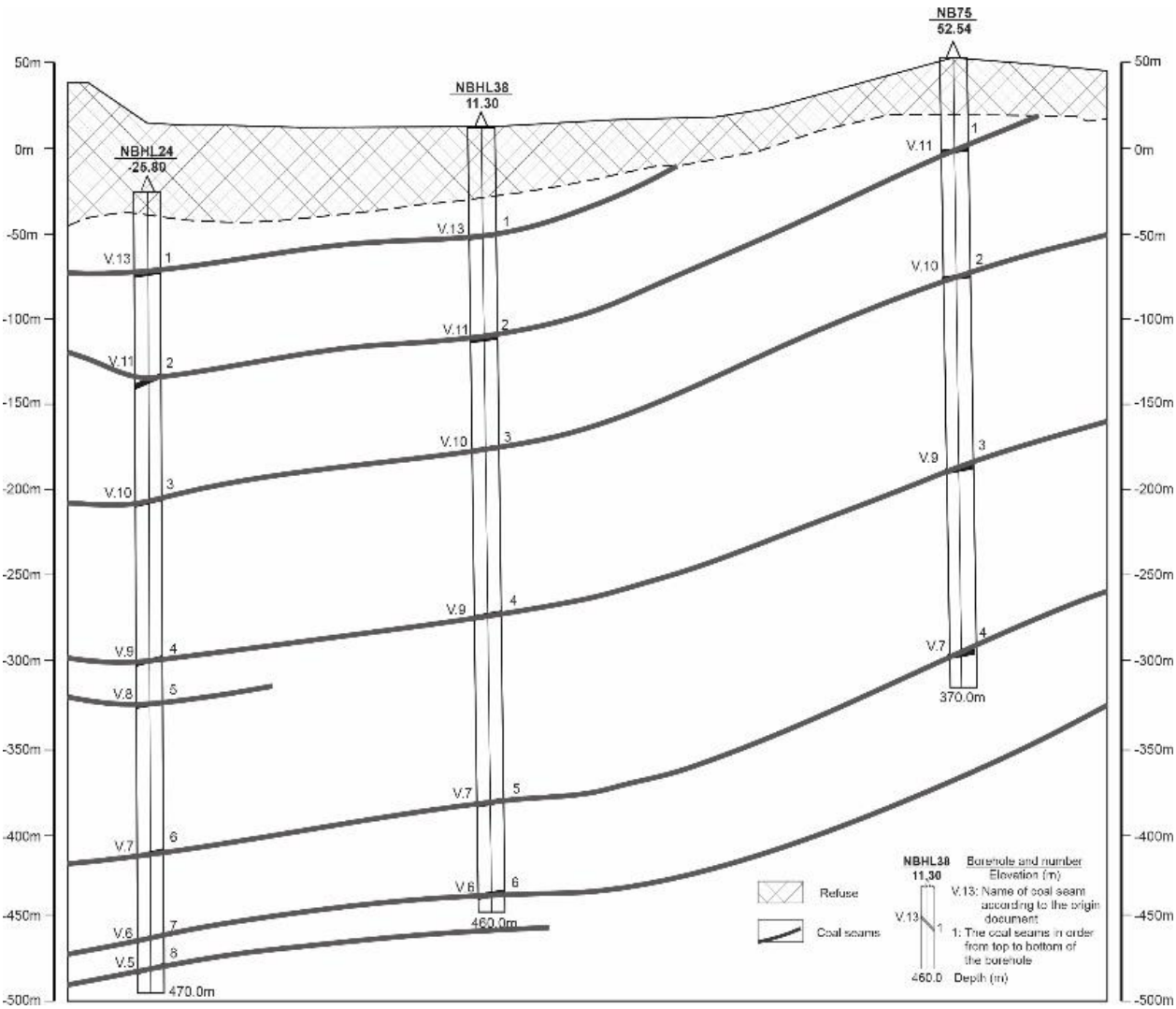

Figure 10. Comparison between the NBHL38 and NB75 boreholes conducted along the T.VIIA cross-section line.

Appendix 5. Results of the comparative parameters between the NBHL38 and NB75 boreholes.

No	Standard borehole (exploration line)	Comparing borehole (exploration line)	Geometric factor (K_{hh})	Standard// Comparing (*)	Sedimentary rock layer factor (M)	Standard// Comparing (**)	Error (Δ)	Standard// Comparing (***)
1	NBHL38 (T.VIIA)	NBHL38 (T.VIIA)	0	1//1	0	1//1	0	1//1
2	NBHL38 (T.VIIA)	NB75 (T.VIIA)	0.026	1//1	0.014	2//1	0.065	2//1

Appendix 6. Results from forecasting the coal seams in the NB75 borehole.

No	Exploration line	Borehole	Coal seam according to the original document(1)	Coordinates of the coal seam in cross-section		Forecasting the coal seam
				X (m)	Y (m)	
1	T.VIIA	NB75	V.11	2243	1197	V.11
2	T.VIIA	NB75	V.10	2243	1123	V.10
3	T.VIIA	NB75	V.9	2245	1009	V.9
4	T.VIIA	NB75	V.7	2247	903	V.7

The method of identifying coal seams is based on blood relationships, especially when differentiating and correlating seams using adjacent boreholes. However, certain exceptional scenarios, such as the omission of a coal seam, can result in misidentification. It is imperative to omit these coal seams from the computational process. Priority should be given to comparing boreholes located within the same cross-section. For boreholes outside this cross-section, their integration mandates a selection centered on the most distinct characteristics.

To optimize the utility of the standard borehole, a comparative analysis was conducted between the borehole NBHL38 and adjacent boreholes not situated along the T.VIIA cross-section line. This was done by adhering to the methodological principle that identifies central relationships. The outcomes of this comparison are consolidated in Appendix 1.

By employing the blood relationship algorithm and designating the borehole NBHL38 as the standard borehole, the calculations, when juxtaposed with results from neighboring boreholes, validate the appropriateness of the linkage method. It is worth noting that only the borehole NB58 utilized the sedimentary rock layer coefficient (*M*) as its comparative metric (Appendix 1). Impressively, across the six instances of comparison, every result was deemed satisfactory, culminating in a 100% success rate.

The correlation methodology employs a standardized approach along each exploration line, using bilateral comparisons from a designated standard borehole. For the T.VIIA cross-section, NBHL38 serves as this standard point. Comparative analyses are conducted to both its immediate right and left within the cross-section. Following this, the recently compared borehole adjacent to the borehole NBHL38 is substituted with the subsequent borehole in the sequence. This process is methodically repeated until all boreholes on the T.VIIA cross-section line have been evaluated (Appendix 2). The outcomes from this approach provide an encouraging perspective on seam linkage (Table 7).

In the process of selecting an appropriate method for comparing coal seams, the minimal values of three key parameters are taken into account: the seam's geometric coefficients (K_{hh}), the sedimentary rock layer coefficient (*M*) and the associated error (*Δ*). Preference is accorded to

Table 7. Summarizing the results of the borehole comparisons along the T.VIIA cross-section line

No	Standard borehole (exploration line)	Comparing borehole (exploration line)	Geometric factor (K_{hh})	Standard// Comparing (*)	Sedimentary rock layer factor (M)	Standard// Comparing (**)	Error (Δ)	Standard// Comparing (***)	Results
1	NBHL38 (T.VIIA)	NBHL38 (T.VIIA)	0	1//1	0	1//1	0	1//1	1//1
2	NBHL38 (T.VIIA)	NB75 (T.VIIA)	0.026	1//1	0.014	2//1	0.065	2//1	2//1
3	NB75 (T.VIIA)	NB76 (T.VIIA)	0.040	1//1	0	1//3	0.066	2//1	2//1
4	NBHL38 (T.VIIA)	NBHL24 (T.VIIA)	0.025	1//1	0.035	1//1	0.050	1//1	1//1
5	NBHL24 (T.VIIA)	NB72 (T.VIIA)	0.077	2//1	0.062	1//1	0.094	2//1	2//1
6	NB72 (T.VIIA)	NBHL08 (T.VIIA)	0.069	1//2	0.025	1//3	0.171	1//2	1//2
7	NBHL08 (T.VIIA)	585 (T.VIIA)	0.261	1//1	0.008	3//1	0.394	2//1	2//2
8	585 (T.VIIA)	KT02 (T.VIIA)	0.280	1//1 (2//2)	0.016	1//4 (2//5)	0.421	1//1 (2//2)	2//3
9	KT02 (T.VIIA)	NBHL23 (T.VIIA)	0.050	1//1	0.037	2//1	0.045	1//1	1//1
10	NBHL23 (T.VIIA)	KT01 (T.VIIA)	0.048	2//1	0.028	1//1	0.177	2//1	2//1
11	KT01(T.VIIA)	SX1903 (T.VIIA)	0.018	1//2	0.011	1//2	0.015	1//2	1//2
12	SX1903 (T.VIIA)	BS12 (T.VIIA)	0.039	1//1	0.017	1//1	0.028	1//1	1//1
13	BS12 (T.VIIA)	580 (T.VIIA)	0.064	1//1	0.224	1//1	0.182	1//1	1//1
14	580 (T.VIIA)	NB69 (T.VIIA)	0.008	1//1	0.008	1//1	0.243	1//1	1//1
15	NB69 (T.VIIA)	582 (T.VIIA)	0.105	1//1			0.026	1//1	1//1
16	582 (T.VIIA)	NBHL21 (T.VIIA)	0.095	1//1			0.366	1//2	1//1
17	NBHL21 (T.VIIA)	NB68 (T.VIIA)	0.198	2//1	0.005	3//1	0.181	3//1	3//1
18	NB68 (T.VIIA)	NBHL02 (T.VIIA)	0.170	1//3	0.008	1//2	0.093	1//2	1//2
19	NBHL02 (T.VIIA)	B575 (T.VIIA)	0.047	1//1	0.029	2//1	0.080	1//1	2//1
20	B575 (T.VIIA)	B569 (T.VIIA)	0.034	1//1	0.046	1//2	0.066	1//1	1//2

scenarios in which the error (Δ) corresponds with either the K_{hh} or M coefficients. Should there be a divergence among all three parameters, the selected method represents a balanced compromise. To elaborate, in instances denoted as comparison cases of 1, 2, 4, 5, 6, 9, 10, 11, 12, 13, 14, 17 and 18, where the error (Δ) is congruent with one of the coefficients - either K_{hh} or M - the option characterized by that specific error (Δ) is chosen. Conversely, in cases 7 and 8, where the parameters exhibit inconsistency, the median value among the trio is selected. Exceptional cases, such as those labeled 7, 19, and 20, necessitate the selection of a coal seam comparison method based on one of the three designated error columns. Furthermore, in the absence of the rock layer coefficient (M), as observed in cases 15 and 16, the decision is predicated on the geometric coefficient (K_{hh}) rather than the error (Δ), given that the latter encapsulates a range of uncertain variables (Table 7).

4.3. Regional application and validation

Extending the analysis to neighboring boreholes (e.g., NBHL24, NB75, NBHL08) maintained high accuracy. Out of 86 comparisons, 74 were correctly identified, yielding an 86.05% overall success rate. Misclassifications primarily occurred in regions with significant faulting or folding, such as in boreholes 585 and KT02, where discontinuities disrupted the stratigraphic sequence. Refinements to the algorithm, including exclusions of problematic seams, resolved these discrepancies (Table 8).

Table 8. Summarizing results from forecasting the coal seams of the boreholes on the T.VIIA cross-section line.

No	Exploration line	Borehole	Coal seam according to the original document(1)	Coordinates of the coal seam in cross-section		Forecasting the coal seam
				X (m)	Y (m)	
1	T.VIIA	NBHL24	V.13	1760	1127	V.13
2	T.VIIA	NBHL24	V.11	1760	1062	V.11
3	T.VIIA	NBHL24	V.10	1760	995	V.10
4	T.VIIA	NBHL24	V.9	1761	897	V.9
5	T.VIIA	NBHL24	V.8	1761	873	V.8
6	T.VIIA	NBHL24	V.7	1762	785	V.7
7	T.VIIA	NBHL24	V.6	1762	736	V.6
8	T.VIIA	NBHL24	V.5	1762	718	V.5
9	T.VIIA	NBHL38	V.13	1960	1148	V.13
10	T.VIIA	NBHL38	V.11	1961	1087	V.11
11	T.VIIA	NBHL38	V.10	1962	1023	V.10
12	T.VIIA	NBHL38	V.9	1964	924	V.9
13	T.VIIA	NBHL38	V.7	1965	816	V.7
14	T.VIIA	NBHL38	V.6	1967	762	V.6
15	T.VIIA	NB75	V.11	2243	1197	V.11
16	T.VIIA	NB75	V.10	2243	1123	V.10
17	T.VIIA	NB75	V.9	2245	1009	V.9
18	T.VIIA	NB75	V.7	2247	903	V.7
19	T.VIIA	NB76	V.10	2460	1181	V.10
20	T.VIIA	NB76	V.9	2462	1081	V.9
21	T.VIIA	NB76	V.7	2465	989	V.7
22	T.VIIA	NB72	V.11	1627	1102	V.11
23	T.VIIA	NB72	V.10	1622	997	V.10
24	T.VIIA	NB72	V.9	1618	923	V.9
25	T.VIIA	NB72	V.7	1617	768	V.7
26	T.VIIA	NBHL08	V.13	1555	1112	V.13
27	T.VIIA	NBHL08	V.11	1555	1082	V.11
28	T.VIIA	NBHL08	V.10	1555	1001	V.10
29	T.VIIA	NBHL08	V.9	1555	905	V.9
30	T.VIIA	585	V.14	1489	1145	V.15
31	T.VIIA	585	V.11	1489	1046	V.12
32	T.VIIA	KT02	V.13	1413	1078	V.14
33	T.VIIA	KT02	V.12	1413	1028	V.13

34	T.VIIA	KT02	V.11	1413	995	V.12
35	T.VIIA	KT02	V.10	1412	971	V.11
36	T.VIIA	KT02	V.9	1409	866	V.10
37	T.VIIA	NBHL23	V.14	1324	1105	V.15
38	T.VIIA	NBHL23	V.13	1324	1058	V.14
39	T.VIIA	NBHL23	V.12	1324	1033	V.13
40	T.VIIA	NBHL23	V.10	1324	962	V.11
41	T.VIIA	NBHL23	V.9	1324	859	V.10
42	T.VIIA	KT01	V.13	1247	1063	V.13
43	T.VIIA	KT01	V.11	1244	984	V.11
44	T.VIIA	KT01	V.10	1244	959	V.10
45	T.VIIA	KT01	V.9	1263	856	V.9
46	T.VIIA	KT01	V.7	1283	756	V.7
47	T.VIIA	SX1903	V.14	1157	1103	V.14
48	T.VIIA	SX1903	V.13	1154	1056	V.13
49	T.VIIA	SX1903	V.11	1142	969	V.11
50	T.VIIA	SX1903	V.10	1140	940	V.10
51	T.VIIA	SX1903	V.9	1131	849	V.9
52	T.VIIA	SX1903	V.7	1128	756	V.7
53	T.VIIA	BS12	V.14	1131	1103	V.14
54	T.VIIA	BS12	V.13	1131	1050	V.13
55	T.VIIA	BS12	V.11	1131	970	V.11
56	T.VIIA	580	V.14	999	1109	V.14
57	T.VIIA	580	V.13	999	1078	V.13
58	T.VIIA	NB69	V.14	967	1110	V.14
59	T.VIIA	NB69	V.13	967	1078	V.13
60	T.VIIA	NB69	V.11	969	954	V.11
61	T.VIIA	NB69	V.9	971	858	V.9
62	T.VIIA	NB69	V.7	972	782	V.7
63	T.VIIA	582	V.14	891	1118	V.14
64	T.VIIA	NBHL21	V.14	817	1125	V.14
65	T.VIIA	NBHL21	V.13	817	1066	V.13
66	T.VIIA	NBHL21	V.11	817	981	V.11
67	T.VIIA	NBHL21	V.7	817	810	V.7
68	T.VIIA	NB68	V.11	678	1055	V.11
69	T.VIIA	NB68	V.7	685	887	V.7
70	T.VIIA	NBHL02	V.13	523	1245	V.13
71	T.VIIA	NBHL02	V.11	523	1127	V.11
72	T.VIIA	NBHL02	V.7	524	954	V.7
73	T.VIIA	NBHL02	V.6	524	891	V.6
74	T.VIIA	NBHL02	V.5	523	858	V.5
75	T.VIIA	B575	V.11	273	1207	V.11
76	T.VIIA	B575	V.7	278	1046	V.7
77	T.VIIA	B575	V.6	279	1000	V.6
78	T.VIIA	B575	V.5	280	957	V.5
79	T.VIIA	B575	V.4	282	916	V.4
80	T.VIIA	B569	V.13	64	1241	V.13
81	T.VIIA	B569	V.11	56	1128	V.11
82	T.VIIA	B569	V.10	48	1042	V.10
83	T.VIIA	B569	V.7	43	970	V.7
84	T.VIIA	B569	V.6	37	896	V.6
85	T.VIIA	B569	V.5	33	846	V.5
86	T.VIIA	B569	V.4	29	797	V.4

The comparative analysis yields distinct correlation outcomes depending on the reference borehole selection. When NBHL08 serves as the standard, an apparent correlation emerges between Coal seam 2 (NBHL08) and Coal seam 1 (585), though subsequent verification reveals this association to be geologically inconsistent. Conversely, using KT02 as the standard establishes a valid alignment between Coal seam 1 in both KT02 and 585 boreholes, which agrees

with the established geological structure and stratigraphic sequence of the mining area (Tables 9 & 10). This comparison demonstrates that the point-to-step verification methodology provides more reliable correlation accuracy (Table 11).

When the 585 borehole acts as the reference point, the predictive results for coal seam connectivity lack assured reliability. Conversely, utilizing the NBHL23 borehole as the standard reveals a notable congruence in the sedimentary rock layer coefficient (*M*). In the specific context of the NBHL23 borehole, the presence of a geological fracture induces displacement, leading to the elimination of the V.11 coal seam. Should this particular seam not be excluded from the analysis, the outcomes of the coal seam comparison are computed as delineated in Table 12.

Following the exclusion of the V.11 coal seam from the NBHL23 borehole analysis, the results reveal consistent correlations between the stratigraphic sequence and the geological framework of the mining area (Tables 13÷17). This demonstrates that the remaining stratigraphic markers provide sufficient resolution for reliable seam identification and structural interpretation.

Table 9. Results of the comparative parameters between the KT02, 585 and NBHL08 boreholes by using the method of determining the relationship to the midpoint with a single-step.

No	Standard borehole (exploration line)	Comparing borehole (exploration line)	Geometric factor (K_{hh})	Standard//Comparing (*)	Sedimentary rock layer factor (M)	Standard//Comparing (**)	Error (Δ)	Standard//Comparing (***)	Results
1	KT02 (T.VIIA)	585 (T.VIIA)	0.280	1//1	0.016	4//1	0.421	1//1	1//1
2	NBHL08 (T.VIIA)	585 (T.VIIA)	0.261	1//1	0.008	3//1	0.295	2//1	2//1

Table 10. Results from forecasting the coal seams in the 585 borehole.

No	Exploration line	Borehole	Coal seam according to the original document(1)	Coordinates of the coal seam in cross-section		Forecasting the coal seam
				X (m)	Y (m)	
1	T.VIIA	585	V.14	1489	1145	V.14
2	T.VIIA	585	V.11	1489	1046	V.11

Table 11. Results of the comparative parameters between the NBHL38, 585 and KT02 boreholes on the T.VII cross-section line by using the method of determining the relationship to midpoint with a single step.

No	Standard borehole (exploration line)	Comparing borehole (exploration line)	Geometric factor (K_{hh})	Standard//Comparing (*)	Sedimentary rock layer factor (M)	Standard//Comparing (**)	Error (Δ)	Standard//Comparing (***)	Results
1	NBHL23 (T.VIIA)	KT02 (T.VIIA)	0.050	1//1	0.037	1//2	0.044	1//1	1//1
2	585 (T.VIIA)	KT02 (T.VIIA)	0.280	1//1	0.016	1//4	0.303	1//1	1//1

Table 12. The comparison results between the NBHL23 and KT02 boreholes do not exclude the V.11 coal seam.

No	Standard borehole (exploration line)	Comparing borehole (exploration line)	Geometric factor (K_{hh})	Standard//Comparing (*)	Sedimentary rock layer factor (M)	Standard//Comparing (**)	Error (Δ)	Standard//Comparing (***)	Results
1	KT02 (T.VIIA)	KT02 (T.VIIA)	0	1//1	0	1//1	0	1//1	1//1
2	KT02 (T.VIIA)	NBHL23 (T.VIIA)	0.050	1//1	0.037	2//1	0.045	1//1	1//1

Table 13. Results from forecasting the coal seams in the NBHL23 borehole do not exclude the V.11 coal seam.

o	Exploration line	Borehole	Coal seam according to the original document(1)	Coordinates of the coal seam in cross-section		Forecasting the coal seam
				X (m)	Y (m)	
1	T.VIIA	NBHL23	V.14	1324	1105	V.15
2	T.VIIA	NBHL23	V.13	1324	1058	V.14
3	T.VIIA	NBHL23	V.12	1324	1033	V.13
4	T.VIIA	NBHL23	V.10	1324	962	V.11
5	T.VIIA	NBHL23	V.9	1324	859	V.10

Table 14. The comparison results between the NBHL23 and KT02 boreholes excluding the V.11 coal seam.

No	Standard borehole(exploration line)	Comparing borehole (exploration line)	Geometric factor (K_{hh})	Standard//Comparing (*)	Sedimentary rock layer factor (M)	Standard//Comparing (**)	Error (Δ)	Standard//Comparing (***)	Results
1	KT02 (T.VIIA)	KT02 (T.VIIA)	0	1//1	0	1//1	0	1//1	1//1
2	KT02 (T.VIIA)	NBHL23 (T.VIIA)	0.029	1//2	0.040	1//2	0.035	1//2	1//2

Table 15. Results from forecasting the coal seams in the NBHL23 borehole excluding the V.11 coal seam.

No	Exploration line	Borehole	Coal seam according to the original document(1)	Coordinates of the coal seam in cross-section		Forecasting the coal seam
				X (m)	Y (m)	
1	T.VIIA	NBHL23	V.14	1324	1105	V.14
2	T.VIIA	NBHL23	V.13	1324	1058	V.13
3	T.VIIA	NBHL23	V.12	1324	1033	V.12
4	T.VIIA	NBHL23	V.10	1324	962	V.10
5	T.VIIA	NBHL23	V.9	1324	859	V.9

Table 16. Results from forecasting the coal seams in the NBHL23 borehole by using a method of determining the relationship to the center.

No	Exploration line	Borehole	Coal seam according to the original document(1)	Coordinates of the coal seam in cross-section		Forecasting the coal seam
				X (m)	Y (m)	
1	T.VIIA	NBHL23	V.14	1324	1105	V.14
2	T.VIIA	NBHL23	V.13	1324	1058	V.13
3	T.VIIA	NBHL23	V.12	1324	1033	V.12
4	T.VIIA	NBHL23	V.10	1324	962	V.10
5	T.VIIA	NBHL23	V.9	1324	859	V.9

Table 17. Summarizing results from forecasting the coal seams of the NBHL23 borehole after adjustment.

No	Exploration line	Borehole	Coal seam according to the original document (1)	Coordinates of the coal seam in cross-section		Forecasting the coal seam		
				X (m)	Y (m)	Along exploration line	After excluding coal seam V.11	Adjustment by determining the relationship to center
1	T.VIIA	NBHL23	V.14	1324	1105	V.15	V.14	V.14
2	T.VIIA	NBHL23	V.13	1324	1058	V.14	V.13	V.13
3	T.VIIA	NBHL23	V.12	1324	1033	V.13	V.12	V.12
4	T.VIIA	NBHL23	V.10	1324	962	V.11	V.10	V.10
5	T.VIIA	NBHL23	V.9	1324	859	V.10	V.9	V.9

On the T.VIIA cross-section line, the BS12 borehole is located to the right of the NB69 borehole and has been accurately identified by the algorithm. Conversely, to the left of the NB69 borehole lies the NBHL21 borehole. The algorithm's identification of this hole was inaccurate due to the omission of the V.13 coal seam (Table 18, Figure 11). By excluding the V.13 coal seam from consideration, the algorithm yields consistent results in coal seam comparisons (Table 19).

Table 18. Comparison results of the NB69 borehole with the NBHL21 and BS12 boreholes on the T.VIIA line using the determining relationship to the midpoint with a jump-step.

No	Standard borehole (exploration line)	Comparing borehole (exploration line)	Geometric factor (K_{hh})	Standard// Comparing (*)	Sedimentary rock layer factor (M)	Standard// Comparing (**)	Error (Δ)	Standard// Comparing (***)
1	NBHL21 (T.VIIA)	NB69 (T.VIIA)	0.042	1//1	0.059	1//3	0.119	1//2
2	BS12 (T.VIIA)	NB69 (T.VIIA)	0.035	1//1	0.068	1//3	0.145	1//1

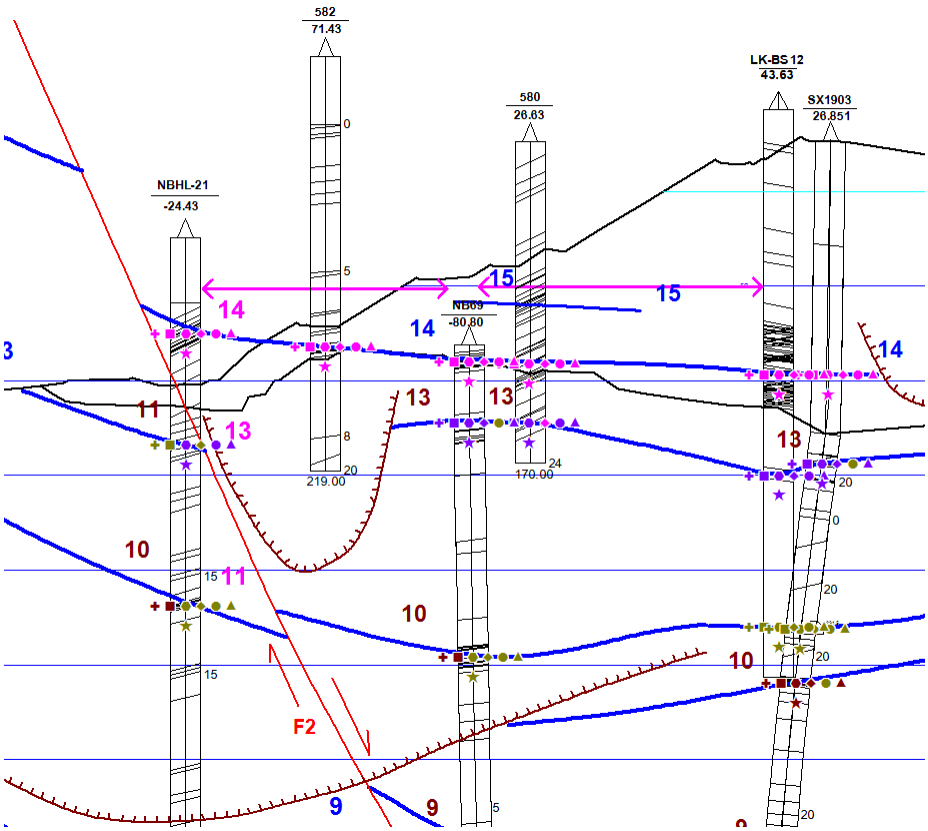

Figure 11. Borehole NB69 is situated between the 582 (with 1 coal seam) and 580 (with 2 coal seams) boreholes on the T.VIIA cross-section line.

Table 19. Comparative results of the NB69 borehole with NBHL21 and BS12 boreholes using the determining relationship to midpoint with a jump-step method, excluding the V.13 coal seam.

No	Standard borehole (exploration line)	Comparing borehole (exploration line)	Geometric factor (K_{hh})	Standard// Comparing (*)	Sedimentary rock layer factor (M)	Standard// Comparing (**)	Error (Δ)	Standard// Comparing (***)	Results
1	NBHL21 (T.VIIA)	NB69 (T.VIIA)	0.065	1//1	0.025	2//1	0.176	1//1	1//1
2	BS12 (T.VIIA)	NB69 (T.VIIA)	0.035	1//1	0.047	1//1	0.212	1//1	1//1

Generally, comparing paired seams along the cross-sectional line may yield discrepancies. However, the effectiveness of the identification process can be enhanced by incorporating various forms of the BLR method. There are 86 cases as a result of the comparison and linkage of the final coal seams for the entire T.VIIA line. After adjustments, all 86 cases were correctly identified with no errors, achieving a 100% accuracy rate.

Specifically, there is a total of 748 cases involved in analyzing the whole Nui Beo mine. The initial data show that while 620 out of 748 cases were correctly identified, the rest 128 were misidentified, leading to an effectiveness rate of 82.89%. After adjusting, 728 out of 748 cases were accurately recognized whereas there were 20 misidentifications, resulting in a success rate of 97.33%. Notably, this rate surpasses the identification outcomes achieved through logistic regression (79.86%) and the RNN method (84.94%) (Hung et al., 2022). The BLR algorithm's superior performance highlights its unique capacity to address coal seam characteristics during nomenclature determination - a capability absent in conventional computational approaches. The lineage-based classification results were subsequently visualized on cross-sections to establish seam linkages.

4.4. Identifying the correlation of the coal seams

Drawing from the sedimentary environment and rock facies within the mining region, the BLR algorithm has proven to be significantly effective in seam linkage tasks. Identification outcomes derived from this method are delineated on the cross-sections of the exploration lines, facilitating the naming conventions for coal seams and their associated sets (Figure 12). To guarantee the precision of coal seam linkages, it is pivotal not only to consider the outcomes from the BLR method but also to acknowledge the intrinsic processes of sedimentary formation. Moreover, the influence of subsequent tectonic movements on the overarching structure of the mining domain cannot be overlooked.

In comparison with the coal seam naming findings presented by Anh (2009), the application of the BLR algorithm in the Nui Beo mining area reveals that 545 out of 748 coal seam positions align, yielding a compatibility rate of 72.85%. Structurally, coal seams connected via the BLR algorithm exhibit a more streamlined and transparent configuration, harmonizing seamlessly with the sedimentary environment. Although the BLR method has achieved initial success in coal seam correlation research, the linking of coal seams encountered in two boreholes that are intersected and displaced by faults still requires human analysis and interpretation. Therefore, BLR method employs algorithms such as the determining relationship to midpoint with a jump-step approach aim to address the aforementioned issue.

In the Nui Beo coal mine, the geological structure shown in the combined data of drilling and tunnel construction is more notably intricate than that presented in the geological report of the

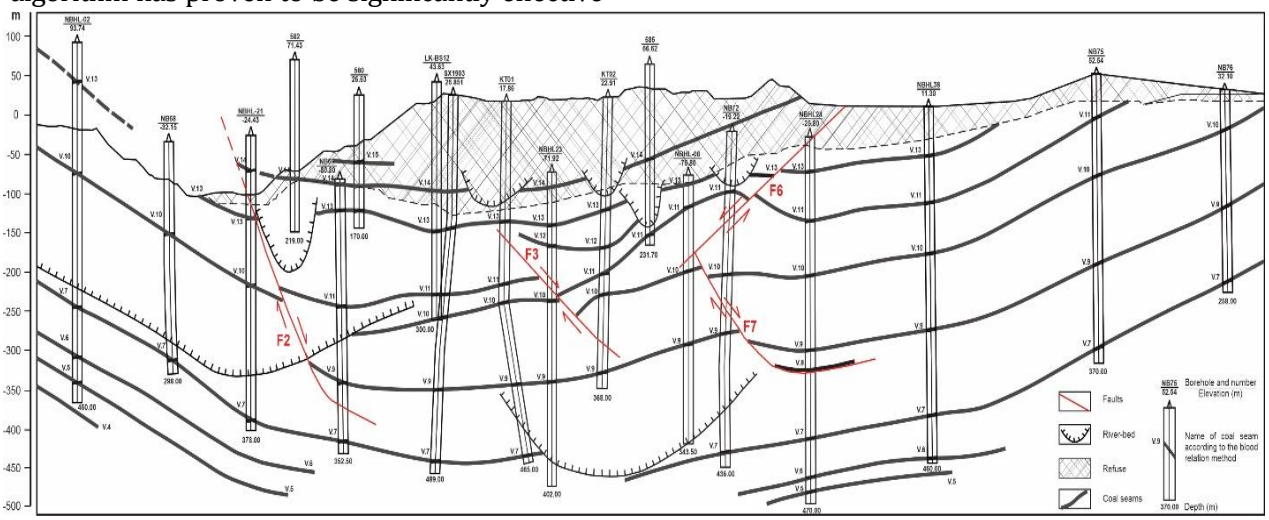

Figure 12. Identifying correlations among coal seams present in the T.VIIA cross-section line.

tunneling project (Hung, 2019). Furthermore, mining activities highlighted the V.12 coal seam, a finding that aligns with this study's observations at the T.VII line cross-section. Discrepancies arose when the actual locations of coal seams in certain boreholes deviated from projections. While exploration documents indicated a coal seam at the NBHL25 borehole, it remained elusive during construction. Anticipated fault sites went unnoticed during the longwall construction phase. Moreover, unforeseen intra-seam faults, particularly at the -220m level not covered in exploration reports, emerged in areas of mechanized mining. To sum up, the coal seam identifications based on the BLR method have offered plausible explanations for specific locales within the mine. These findings stand validated by subsequent exploratory drills and mining endeavors.

5. Conclusion

Using the BLR approach, the investigation that identifies and connects the coal seams in the Nui Beo mining region reveals some subsequent conclusions:

1) The comparison between the schematic representation of coal seam linkage derived from the BLR algorithm and that of established linkage from exploration records shows a congruence of 72.57%, suggesting that the mine's structural delineation, as depicted in earlier documentation, offers foundational guidance and sets the orientation for the algorithmic coal seam linkage approach.

2) The BLR approach does not anchor its analysis of the specific traits of the coal seam due to its distinction, resulting in a marked improvement in identification accuracy by 97.33%, which outperforms feature-based methods such as logistic regression (70.87%) and the RNN method (84.94%). Despite the superior performance of the blood relation method, it has a residual error of 2.67%. Still, this stands as the most optimal and acceptable outcome when leveraging algorithms for coal seam linkage endeavors.

3) In contrast to conventional seam linkage techniques, the BLR algorithm produces more geologically coherent correlations within the Nui Beo mining zone. The resulting connections demonstrate both greater interpretative clarity and improved alignment with paleo-depositional conditions. These findings reinforce the critical principle that accurate seam linkage requires thorough understanding of the original coal-forming environment.

4) This study demonstrates the critical importance of advanced mathematical methods in geological application, specifically for coal seam identification, correlation and linkage. The methodological framework developed here achieves two significant outcomes: (1) substantial reduction of mining risks through improved seam identification accuracy and (2) reliable quantification of extractable reserves for individual seams in the Nui Beo deposit. These advancements provide both practical safety benefits and essential economic data for mine planning and resource management.

Contributions of authors

Hung The Khuong - methodology, writing, review, editing and supervision; Toan Thi Ta - data collection and processing, writing and editing; Hien Thi Pham - data collection, map creation, writing and editing.

References

Anh, P. T. (ed.) (2009). *The report delineates the transformation in coal reserve levels and the grading of coal resources pertaining to the Ha Lam mine*. Archived at the Vietnam National Coal and Mineral Industries Group (Vinacomin), 105 p (in Vietnamese).

Crook, A. W. (1974). Lithogenesis and geo-tectonics: the significance of compositional variations in flysch arenites (graywackes), in Dott, R. H. and Shaver, R. H., eds., Modern and ancient geosynclinal sedimentation. *SEPM Special Publication,* 19, 304-310. https://doi.org/10.2110/pec.74.19.0304.

Dickinson, W. R., Suczek, C. A. (1979). Plate tectonics and sandstone compositions. *American Association of Petroleum Geologists Bulletin,* 63, 2164-2182. https://doi.org/10.1306/2F9188FB-16CE-11D7-8645000102C1865D.

Dickinson, W. R., Valloni, R. (1980). Plate settings and provenance of sands in modern ocean basins. *Geology,* 8, 82-86. https://doi.org/10.1130/0091-7613(1980)8%3C82:PSAPOS%3E2.0.CO;2.

Duan, H., Xie, W., Zhao, J., Jia, T. (2021). Sequence stratigraphy and coal accumulation model of the Taiyuan Formation in the Tashan Mine, Datong Basin, China. *Open Geosciences*, 3(1), 1259-1272. http://dx.doi.org/10.1515/geo-2020-0303.

Dyke, M. V., Klemetti, T., Wickline, J. (2020). Geologic data collection and assessment techniques in coal mining for ground control. *International Journal of Mining Science and Technology,* 30(1), 131-139. https://doi.org/10.1016/j.ijmst.2019.12.003.

Einsele, G. (2020). *Sedimentary Basins, Evolution, Facies and Sediment Budget*. Springer-Verlag Berlin Heidelberg. https://doi.org/10.1007/978-3-662-04029-4.

Freedman, D. A. (2009). *Statistical models: theory and practice*. Cambridge University Press, 12 p.

Hou, H., Shao, L., Tang, Y., Li, Y., Liang, G., Xin, Y., Zhang, J. (2023). Coal seam correlation in terrestrial basins by sequence stratigraphy and its implications for paleoclimate and paleoenvironment evolution. *Journal of Earth Science,* 34, 556-570. https://doi.org/10.1007/s12583-020-1069-4.

Hung, K. T., Phuong, N., Cuc, N. T., Sang, P. N., Tuyen, N. D. (2021). Identifying Correlation of Coal Seams in the Tien Hai Area, Northern Vietnam by Using Multivariate Statistic Methods. *Inżynieria Mineralna - Journal of the Polish Mineral Engineering Society,* 2(46),129-148. http://doi.org/10.29227/IM-2021-02-11

Hung, K. T., Toan, T. T., Tuyen, N. D. (2022). Identifying the correlation of coal seams in Nui Beo mine, Quang Ninh province using logistic regression and artificial intelligence methods. *Proceedings of the 5th National Conference on Sustainable Earth, Mine, Environment Creative,* 305-317 (in Vietnamese). http://doi.org/10.15625/vap.2022.0184.

Hung, K. T., Tuyen, N. D. (2023). Identifying the coal seams and their sedimentary environments in the Nui Beo mine, Quang Ninh province using K-means and regression methods. *Science & Technology Development Journal - Science of the Earth & Environment,* 6(2), 583-599 (in Vietnamese). https://doi.org/10.32508/stdjsee.v6i2.692.

Hung, L. (ed.) (1996). *Report on Geological and Mineral resource mapping at 1:50.000 scale of the Hon Gai-Cam Pha sheet group*. The Vietnam Geological Department (VGD), Hanoi, 58 p.

Hung, N. M. (ed.) (2019). *Report on the results of the exploration of Ha Lam coal mine, Ha Long, Quang Ninh*. Ministry of Natural Resources and Environment Vietnam, 110 p (in Vietnamese).

Konstantinov, A. R. (1968). *Ispareniye v prirode (Evaporation in nature)*. Leningrad, Russia, Hydrometeorological publishing, 532 p (in Russian).

Potter, E. (1978). Petrology and chemistry of modern big river sands. *Journal of Geology,* 86, 423-449.

Schwab, L. (1975). Framework mineralogy and chemical composition of continental margin-type sandstone. *Geology,* 3(9), 487-490. https://doi.org/10.1130/0091-7613(1975)3%3C487:FMACCO% 3E2.0.CO;2.

Steinhaus, H. (1956). Sur la division descorps matériels en parties. *Bulletin del'Académie Polonaise des Sciences,* 3(12), 801-804.

Valloni, R., Maynard, J. B. (1981). Detrital model of Recent deep-sea sands and their relation to tectonic setting: A first approximation. *Sedimentology*, 28, 75-83. https://doi.org/10.1111/j.1365-3091.1981.tb01664.x.

Zhifei, L., Yingchun, W., Shuzheng, N., Xu, J., Rongfang, Q., Daiyong, C. (2019). The differences of element geochemical characteristics of the main coal seams in the Ningdong coalfield, Ordos Basin. *Journal of Geochemical Exploration,* 202, 77-91. https://doi.org/10.1016/j.gexplo.2019.03.018.

Srivastava, A. K., Agnihotri, D. (2013). Coal seam correlation of an Indian Gondwana coalfield: A palaeobotanical perspective. *International Journal of Coal Geology,* 113, 88-96. https://doi.org/10.1016/j.coal.2012.06.009.

Shi, J., Zeng, L., Dong, S., Wang, J., Zhang, Y. (2020). Identification of coal structures using geophysical logging data in Qinshui Basin, China: Inestigation by kernel Fisher discriminant analysis. *International Journal of Coal Geology,* 217, 103314. https://doi.org/10.1016/j.coal.2019.103314.

Li, Y., Shao, L., Fielding, C. R., Wang, D., Mu, G. (2021). Sequence stratigraphy, paleogeography and coal accumulation in a lowland alluvial plain, coastal plain and shallow-marine setting: Upper Carboniferous-Permian of the Anyang-Hebi coalfield, Henan Province, North China. *Palaeogeography, Palaeoclimatology, Palaeoecology,* 567, 110287. https://doi.org/10.1016/j.palaeo.2021.110287.